

Highly Sensitive Real-Time Isotopic Quantification of Water by ATR-FTIR

Cei B. Provis-Evans, Elliot H. E. Farrar, Matthew N. Grayson, Ruth L. Webster,* and Alfred K. Hill*



Cite This: *Anal. Chem.* 2020, 92, 7500–7507



Read Online

ACCESS |



Metrics & More

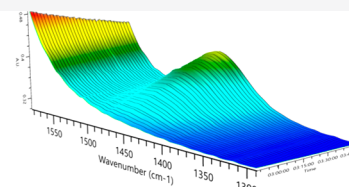


Article Recommendations



Supporting Information

ABSTRACT: A method has been developed to reliably quantify the isotopic composition of liquid water, requiring only immersion of a “ReactIR” probe in the sample under test. The accuracy and robustness of this method has been extensively tested using a deuterium/protium system, and substantial improvements in sensitivity were obtained using highly novel chemical signal amplification methods demonstrating a standard deviation of 247 ppb D (a δD of 1.6 ‰). This compares favorably with other more costly and time-consuming techniques and is over 20 times more sensitive than any previously published FTIR study. Computational simulations of a model system match the experimental data and show how these methods can be adapted to a tritium/protium system.



- In-line ^2H -atom quantification *ReactIR*
- Signal amplification using EtOH 1.60 ‰
- ^2H as a proxy for ^3H *evidenced by DFT*

Tritium is one of the most challenging radio-isotopes to measure and to remove from waste streams.¹ It is harmful in very low concentration, and it is present in experimental fusion reactors such as ITER and the Joint European Torus (JET) and in the Fukushima postaccident wastewater.² The conventional technique, liquid scintillation counting (LSC), is an off-line method, and there is no effective online detection method.^{3,4} In this work we explored the potential of an in situ and online ATR-FTIR measurement for deuterium in water and used molecular modeling to generate simulated IR spectra to understand how the method would translate for aqueous tritium detection.

Measurement of deuterium in water is important for paleoclimatology,⁵ medical and biochemical studies,⁶ forensic studies of the movement of living things,⁷ and ecological and geochemical studies of water origin.^{8,9} For water, the stable isotopologues of interest are $^1\text{H}_2^{16}\text{O}$, $^1\text{H}^2\text{H}^{16}\text{O}$ and $^1\text{H}_2^{18}\text{O}$.

When isotopic ratios vary by very small amounts, the variance is quantified using δ notation. For water the D/H ratio is given relative to Vienna Standard Mean Ocean Water (VSMOW) which is 155.76 ± 0.1 ppm, expressed permille as per eq 1 below.¹⁰ The sensitivity of the technique given in terms of its standard deviation (SD) can be converted between ppm and δD basis using eq 2.

$$\delta D = \left(\frac{R_{\text{sample}}}{R_{\text{standard}}} - 1 \right) \times 1000 \quad (1)$$

$$\text{SD}_{\delta D} = \frac{1000}{156} \text{SD}_{\text{ppm}} \quad (2)$$

where R is the ratio of D/H.

Quantification of isotopic abundance for tritium (^3H or T) is typically undertaken using liquid scintillation counting (LSC). In this technique, beta decay of ^3H to ^3He excites a scintillation medium producing pulses of light.¹¹ While highly sensitive, this method is time-consuming and requires off-line processing. ^3H mass spectrometry provides greater sensitivity but is not suitable as an online test.¹²

Tritium concentration can be expressed in tritium units (TU), which is the ratio of 10^{-18} ^3H to ^1H and ^2H or by its activity in Bq/kg.¹³ Equivalence of absolute concentration in ppm to the other units is $1 \text{ ppm } T = 10^{12} \text{ TU} = 118 \text{ GBq/kg}$. In this work quantification of deuterium has been considered as a proxy for tritium due to restrictions on its use.

Unstable isotopes can be detected through their emission of ionizing radiation, but stable isotopes do not decay and therefore can only be quantified by their subtle chemical differences. Modern techniques include mass spectrometry (MS),^{14–16} vibrational optical methods using either single wavelengths¹⁷ (e.g., CRDS¹⁸ and OA-ICOS¹⁹), or the full IR spectrum (FTIR).^{14,19}

MS is the most commonly used technique, often enhanced by ionization and in-line sample preparation methods.^{20,21} The SD for deuterium quantification has been quoted between 2 and 5 ‰.¹⁶ Drawbacks include the high cost, large equipment

Received: December 20, 2019

Accepted: April 29, 2020

Published: April 29, 2020



size, and analysis of water requires conversion to H₂ and HD.^{20,22–24}

Fourier transform infrared spectroscopy (FTIR) uses infrared light to explore the vibrational characteristics of molecules. It is not generally used as a quantitative tool although a recent study using an FTIR flow cell detected deuterium in water with an SD of 38.54 ‰ utilizing an O–D stretching absorption peak at 2504 cm⁻¹.^{9,25}

FTIR has a number of advantages over the other analytical methods. It can measure aqueous samples in situ, without derivatization or vaporization. The attenuated total reflectance (ATR) method allows for further simplification as the optical path length does not need to be considered.

EXPERIMENTAL SECTION

ATR-FTIR experiments used a Mettler Toledo ReactIR 15 instrument, a “DiComp” diamond ATR cell with a silver halide optical fiber, or a PerkinElmer Spectrum 100. Temperature and pH were measured using a calibrated Hanna Instruments HI 83141 pH meter/temperature probe, calibrated at pH 10 and 4 buffer solutions. Robustness solutions adjusted with HCl for pH 2 and NaOH for pH 10. Experimental and calibration solutions used deuterium depleted water (<1 ppm D), deuterium oxide (99.95% D atom), or deionized water. Chemicals were from Sigma-Aldrich, Alfa Aesar or Fisher. DI water was obtained by reverse osmosis. Details on the experimental protocol for calibration and determinations are given in the Supporting Information (SI).

All computed structures were optimized by DFT calculations using Gaussian16 (revision A.03;²⁶ see the SI for full reference) with the B3LYP-D3(BJ) density functional,^{27–29} def2-TZVPP basis set,³⁰ and the IEF-PCM³¹ to account for the effect of water as solvent. Temperature (298.15K) and concentration-corrected (1 mol/L) quasiharmonic free energies were calculated with GoodVibes.³²

RESULTS AND DISCUSSION

The study first sought to develop a testing methodology to maximize sensitivity and establish important metrics such as the limits of detection and of quantification. Improvements in sensitivity were produced through chemical signal amplification techniques and molecular modeling was used to gain further insight and to predict tritium spectra. Details on the experimental protocol for calibration and determinations, along with details regarding density functional theory (DFT) calculations are given in the ESI.

An initial investigation was carried out on the standard ATR-FTIR instrument. Resolution between O–H/O–D stretching absorbances (3380 and 2470 cm⁻¹, respectively), as well as H₂O, HDO, and D₂O scissoring absorbances (1660 cm⁻¹, 1460 and 1200 cm⁻¹) was good, and ATR-FTIR appeared suited to this sort of isotopic analysis (spectrum A, Figure 1). These results were then repeated with the ReactIR instrument. While offering better resolution, the ReactIR is constrained by its flexible silver halide optical fiber which is opaque above 3000 cm⁻¹ and in practice any absorbances above 1900 cm⁻¹ were not visible. It is therefore not possible to look at absorptions at wavenumbers higher than this, including O–H/O–D stretching peaks.³³ Consequently, the scissoring vibrational mode region (ca. 1650–1200 cm⁻¹) was of most interest (spectrum A, Figure 1).

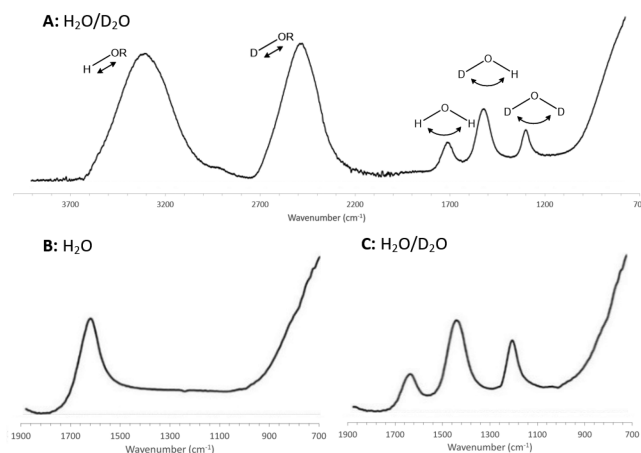


Figure 1. (A) standard ATR-FTIR instrument with 50:50 H₂O:D₂O mix. R = H or D; (B) H₂O scissoring peak observed at 1640 cm⁻¹ with ReactIR; (C) scissoring peaks for H₂O (1645 cm⁻¹), HDO (1450 cm⁻¹), and D₂O (1210 cm⁻¹) with ReactIR (50:50 H₂O:D₂O).

The spectra obtained indicate that the instrument is capable of resolving between protic water, singly deuterated water and doubly deuterated water such that quantification of deuterated species is potentially possible (spectrum C, Figure 1).

Resolution between the species shown in spectrum C of Figure 1 suggests that quantitative detection of deuterium at low levels is possible by evaluating the magnitude of the HDO scissoring peak at 1450 cm⁻¹.

The first experimental step was to construct a thermostatically controlled environment in which to carry out the experiments, with an atmosphere of dry N₂ maintained over the test solution at all times to minimize proton exchange with ambient water vapor (see the SI). A fixed quantity of deionized (DI) water was added, and then known quantities of a 124 504 ppm deuterium atom standard made from D₂O and deuterium depleted water were added sequentially to produce a series of five spectra with between 156 and 9367 ppm deuterium atom. All ppm values are quoted as an absolute ratio of D/H. A systematic exploration of the various options available within the software for quantitating deuterium by evaluating the peak at 1450 cm⁻¹ was conducted; peak height (spectrum A, Figure 2), area relative to zero (not shown) or peak area to a specified baseline on the spectrum (spectrum B, Figure 2). The subtraction of a baseline taken directly from the spectrum as shown in spectrum B, Figure 2, allows much of the variation in the height of successive spectra to be mitigated and therefore analytical noise to be suppressed.

A linear regression was produced for each of the various peak evaluation methods using the five spectra previously collected, relating the deuterium concentration with the height or area of the HDO scissoring peak. Coefficients of determination (*R*²) were calculated from these linear regressions, and it was apparent from these that integration to give the area under the peak relative to a two-point baseline (i.e., spectrum B, Figure 2) was significantly superior over other options.

The influence of interfering peaks and baseline variability was limited by optimization of both the limits between which the peak is integrated and the two points between which the baseline is drawn. This was achieved with the use of an algorithm which varied each of the four parameters (integration start/finish and baseline start/finish), integrated

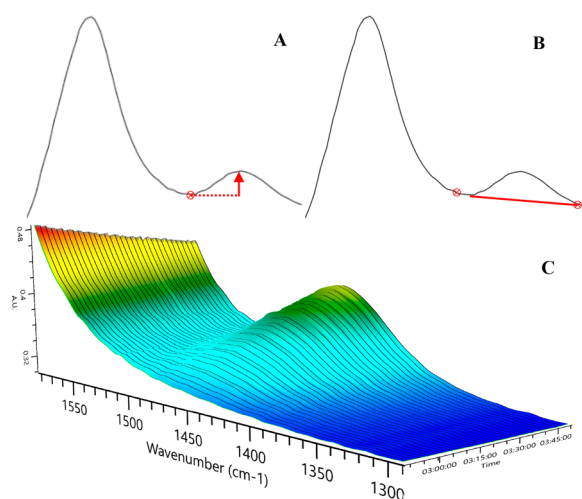


Figure 2. (A) Height of the peak relative to a fixed point, (B) integration of the area under the peak between two points relative to a baseline. (C) spectral changes with increasing deuterium concentration in the HDO region.

the five spectra based on these parameters, produced a linear regression from the area obtained and then recorded the R^2 value. A model of a quantification method was written (see the SI) involving the production of a five-point calibration curve using the integration parameters with the highest R^2 value, and the curve used to quantify the deuterium concentration of unknown samples. This will be referred to as “method 1”.

Deuterium standards used in the method for the following experiments were prepared from commercially obtained D_2O and D depleted H_2O . Traceable to the Vienna Standard Mean Ocean Water (VSMOW) deuterium standard was not considered to be necessary given that the experiments consider the potential utility of the ATR-FTIR technique as a means to quantify deuterium atom concentration, rather than to validate a specific quantification method for unknown samples. Given that the standards were not prepared from certified reference standards, the uncertainties associated with their preparation were not calculated explicitly as any calculations would not be able to consider the uncertainty associated with the D concentration of the commercially obtained D_2O and H_2O . Instead, the uncertainty was assessed practically within the method validation, with any unacceptably high uncertainty expected to give failures in the accuracy and precision of experiments.

The optimized procedure obtained one spectrum every minute (256 scans), with deuterium concentrations averaged from four of these spectra to obtain one determination. This method provided an instrumental standard deviation (SD) of 43 ppm D (approximately 268 ‰ δD).

METHOD VALIDATION

In order to demonstrate that method 1 is suitable for quantification of deuterium concentration and to determine the limitations of the method, a validation protocol was developed and undertaken (see the SI for protocol and data with a summary in Table 1 below). Acceptance criteria were set with reference to ICH advice for the validation of pharmaceutical analytical methods³⁴ and from Shabir.³⁵ Validations of other FTIR quantification methods were also inspected for comparison and acceptance criteria adjusted accordingly.³⁶

Table 1. Summary of Method Validation Experiments Conducted on Method 1

experiment	criteria, acceptance	data obtained	pass/fail
accuracy/linearity	distance from target, <2 SD	All samples fell within 2 SD	pass
	$R^2, \geq 0.9990$	0.9999	pass
precision-repeatability	RSD, $\leq 2.0\%$	1.6%	pass
	RSD, $\leq 4.0\%$	level 3 = 3.5%	pass
intermediate precision		level 4 = 3.0%	pass
LOD		137 ppm D	N/A
LOQ		156 ppm D	N/A
robustness	temperature, <2.5% deviation	± 2 °C, > 2.5%	Fail
		± 5 °C, > 2.5%	fail
	pH, <2.5% deviation	pH 2 ^a <2.5%	pass
		pH 10 ^b <2.5%	pass
	ionic strength, <2.5% deviation	1%, < 2.5%	pass
		6%, > 2.5%	fail
	remove N_2 , <2.5% deviation	<2.5%	pass
instrumental SD	60 repeat determinations	43 ppm D	N/A

^aAdjusted with HCl. ^bAdjusted with NaOH.

The data obtained demonstrates that the ReactIR instrumentation under test is suitable for the quantification of deuterium in water with instrumental SD of 43 ppm D. The technique is robust to changes in pH and up to 1% ionic strength between calibration and quantification and is not robust to differences in temperature between calibration and quantification, although this can be overcome by calibrating the instrument at a given temperature. The straightforward nature of the method added to the lack of sample preparation suggests that field applications would be feasible with this technique, especially considering that extreme changes in temperature, pH, and ionic strength are unlikely to occur during environmental sampling between calibration and testing.

To evaluate the rapid response required for online application in a flowing system, rapid stepped addition of 124 504 ppm D standard was made (calibration per method 1), and the instrument response is shown in Figure 3.

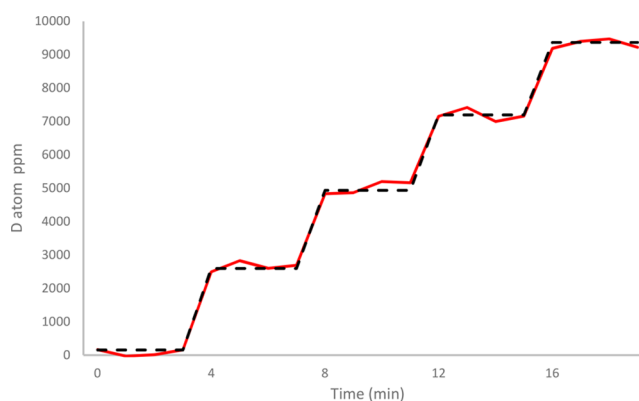


Figure 3. Deuterium concentration over time (red line), versus calculated nominal deuterium atom added to system (black dashed line) for stepped concentration changes.

SIGNAL AMPLIFICATION

The systemic evaluation of method 1 conducted above shows that ATR-FTIR is a feasible technique for the swift, online and nondestructive quantification of low levels of deuterium in water. However, significant improvement in sensitivity is required if this technique is to become competitive with MS or laser based optical techniques, or to be applied to systems where concentrations are much lower. In the case of fusion reactor applications, the concentration of tritium in water arising from the exhaust detritiation systems ranges from 25–250 ppb³⁷ and other applications such as effluent from fission reactors and contaminated water from Fukushima are many orders of magnitude below this.³⁸

In order to improve the sensitivity, it would be desirable to find another absorbance peak responsive to deuterium which is both better resolved and larger than the HDO scissoring peak. The transparency limitations of the silver halide optical fiber mean that the O–H/O–D stretching frequencies of HDO (3350 and 2480 cm⁻¹) are not usable with this instrument so an investigation into other molecules with labile protons was undertaken to see if a well resolved, deuterium-responsive peak could be identified. For each experiment, 5 mL of methanol, ethanol, 80% w/v phenol in water, isopropyl alcohol (IPA), ethylene glycol, 70% w/v ethylamine in water, or acetic acid were placed in the test vessel in sequence and spectra were collected. Then, 400 μL of D₂O was then added to each potential signal amplifier, and the spectra compared. Methanol and ethanol displayed promising deuterium responsive absorbances (spectra A and B, Figure 4), while the amine, acid, and more complicated alcohols showed correspondingly more complex and less well resolved changes upon the introduction of deuterium (see the SI).

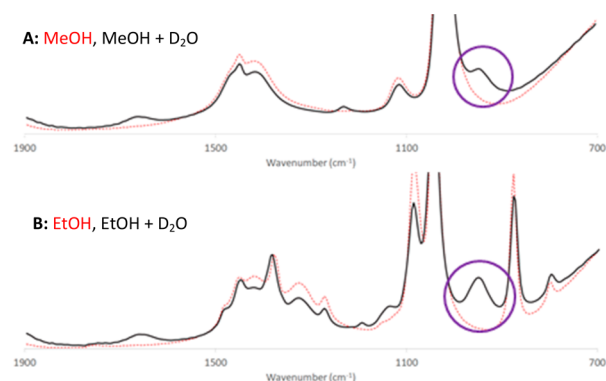


Figure 4. Spectra collected of 5 mL of various organic compounds (dashed red) and the same compounds after the addition of 400 μL of D₂O (black). A, methanol; B, ethanol.

Methanol shows a growth in two peaks on the addition of deuterium; the small, well resolved absorbance at 1230 cm⁻¹ (spectrum A, Figure 4, labeled in green) and the much larger but poorly resolved peak at 945 cm⁻¹ (spectrum A, Figure 4, labeled in purple). Ethanol also shows a corresponding small absorbance at 1195 cm⁻¹ (spectrum B, Figure 4, labeled in green); however, the larger peak at 950 cm⁻¹ (spectrum B, Figure 4, labeled in purple) is both larger and better resolved than seen with methanol. An investigation was conducted to understand whether quantification using either of these well resolved absorbances represents an improvement over method 1. Initially, the calibration parameters outlined in method 1 were used (see the SI), which stipulate the addition of up to 400 μL of water to 5 mL of natural D abundance ethanol and methanol. This gave a somewhat inferior R² value of 0.9986 for the methanol peak at 1230 cm⁻¹ and 0.9995 for the ethanol peak at 950 cm⁻¹. The quantity of water used to prepare the standard had the secondary effect of diluting the linear response of the alcohol peaks to deuterium concentration since some of the deuterium forms HDO with the water from the standard solution. To minimize this loss of linearity, the ethanol calibration was repeated with ten times less standard. This new calibration between 156 and 1143 ppm D yielded a R² of 1.0000, which appears to show that the loss of linearity induced by added water is not significant at this level and also demonstrated an improvement in the analytical noise over method 1, with an SD of 3.8 ppm.

To further explore the potential of this signal amplification method, a lower concentration standard of 1992 ppm D was used, and again this was added at a tenth of the volumes stipulated in method 1 to give a calibration between 156 and 170 ppm D (Table 2). The standard deviation of this method with ethanol as a signal amplifier is 1.60 ‰ δD (247 ppb), and the LOD calculated using the limit of the blank method enumerated above is 5.36 ‰. This is significantly more sensitive than the LOD of 1212.00 ‰ for the pure water method (calculated from the same data which gives 137 ppm D quoted previously). It is clear that the deuterated ethanol absorbance at 950 cm⁻¹ is significantly more sensitive to deuterium concentration than the HDO absorbance at 1450 cm⁻¹. Direct comparison of quantification using the three solvents is shown in Table 2 (see the SI for data).

COMPUTATIONAL SIMULATION OF IR SPECTRA

The potential extrapolation of these methods for the quantification of tritium was studied by analysis of a series of computationally simulated IR spectra (double harmonic approximation), generated by Gaussian16 (Revision A.03),²⁶ optimization and frequency calculations (see the SI) on

Table 2. Summary of Calibration Experiments Comparing the Pure Water Method with Simple Alcohols^a

solvent	cal. range (156 – x ppm D)	R ^{2b}	SD ^c (ppm D)	tritium equiv. (GBq/kg) ^d	LOD (‰ δD)
H ₂ O	9367	0.9999	42.60	5026.80	1212.00
H ₂ O	292	0.5276			
MeOH	9367	0.9986	53.12	6268.16	
EtOH	9367	0.9995			
EtOH	1143	1.0000	3.80	448.40	
EtOH ^e	170	0.9999	0.25	29.50	5.30

^aEthanol shows a substantial improvement in the SD of repeated determinations and LOD. Peak analyzed 1450 (water), 1230 (MeOH), and 950 cm⁻¹ (EtOH). ^bR² of 5-point calibration. ^cStandard deviation of 60 repeats. ^dTritium activity equivalents for illustration only, calculated by multiplying SD of D determinations in ppm by 118 GBq kg⁻¹. ^eAll other samples in the table were averaged over 4 min.

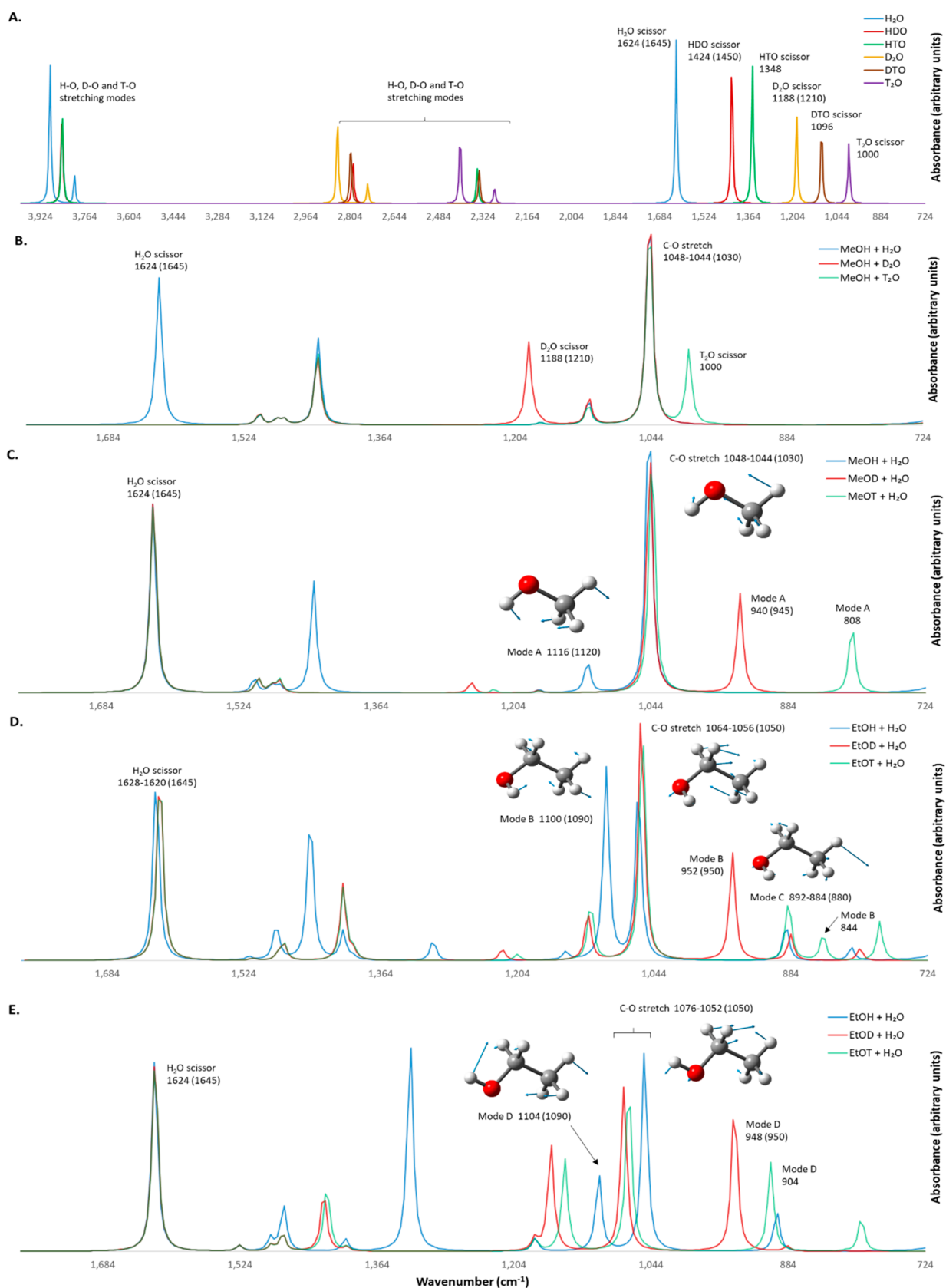


Figure 5. Simulated IR spectrum (B3LYP-D3(BJ)/def2-TZVPP/IEF-PCM(water)) for (A) isotopologues of water; (B) methanol with isotopologues of water; (C) isotopologues of methanol with water; (D) isotopologues of gauche-ethanol with water; (E) isotopologues of antiethanol with water. Experimental frequencies and vibrational modes (water removed) included where available.

isolated H₂O, HDO, D₂O, HTO, DTO, T₂O, and all combinations of ROX + X₂O (R = Me and Et and X = H, D, and T). Full details of the computational methods and explanation of additional considerations regarding proton exchange, hydrogen-bonding, and anharmonicity in the computed spectra, are found in the SI. Additionally, a series of other molecules were tested as potential signal amplifying molecules, but ethanol was found to provide the best combination of sensitivity and practicality (see the SI).

The simulated spectra for H₂O, HDO, and D₂O (spectrum A, Figure 5) were found to match very closely with the experimental spectra (Figure 1), in particular the scissoring vibrational mode, which is ideal given the limits of the ReactIR instrument to absorbances only below 1900 cm⁻¹. Based on the HTO, DTO, and T₂O spectra (spectrum A, Figure 5), the scissoring vibrational modes for these species should occur at approximately 1348, 1096, and 1000 cm⁻¹, respectively. Importantly, these are distinct from each other and from the H₂O scissoring mode, and hence the ReactIR instrument should theoretically be capable of resolving between protic water, singly tritiated water, and doubly tritiated water. This would allow quantitative detection of tritium by evaluation of the magnitude of the HTO scissoring peak at 1000 cm⁻¹, analogous to method 1.

The only significant difference between the simulated MeOH + X₂O spectra (spectrum B, Figure 5) was the movement of the X₂O scissoring mode from 1624 cm⁻¹ in H₂O to 1188 cm⁻¹ in D₂O and 1000 cm⁻¹ in T₂O. This shows that the well resolved absorbance at 1230 cm⁻¹ (spectrum A, Figure 4, labeled in green) is in fact due to the pure D₂O scissoring vibrational mode, which is also responsible for the small absorbance at 1195 cm⁻¹ in the experimental ethanol spectrum (spectrum B, Figure 4, labeled in green). Accordingly, analogous peaks representing the HTO and T₂O scissors would be expected to appear in the tritiated methanol and ethanol spectra at around 1348 and 1000 cm⁻¹, respectively; however, these are likely to be hidden among other absorbances in these regions (just as the peak due to the HDO scissor is hidden under the broad absorbance from 1300 to 1600 cm⁻¹), making accurate evaluation difficult.

In the simulated spectra for MeOX + H₂O (spectrum C, Figure 5), a strong peak due to the C–O methanol stretch was observed at 1044–1048 cm⁻¹ for all three isotopologues, corresponding to the strong absorbance in the experimental spectrum at 1030 cm⁻¹ (spectrum A, Figure 4). In protic methanol, an absorbance due to vibrational mode A was observed at 1116 cm⁻¹, on the higher frequency side of the C–O stretch, which corresponds to the small absorbance at 1120 cm⁻¹ in the experimental spectrum. In deuterated methanol this peak shifted down to 940 cm⁻¹, onto the lower frequency side of the C–O stretch, explaining the appearance of the larger peak at 945 cm⁻¹ (spectrum A, Figure 4, labeled in purple) and the corresponding decrease in intensity of the 1120 cm⁻¹ absorbance. Extrapolating this trend to tritiated methanol would predict a further shift of mode A down to approximately 808 cm⁻¹, although in practice this peak may be difficult to resolve from the broad absorbance seen at the low frequency end of the experimental spectrum (as also indicated in the hydrogen-bonded and anharmonic spectra (Figures S3B and S4B, respectively)).

Ethanol exists in two energetically similar conformations: anti and gauche. While the gauche conformation is marginally higher in energy ($\Delta G = 0.073$ kcal mol⁻¹), it also exhibits a

double degeneracy over the anti conformation,³⁹ meaning both conformations are significantly populated overall. Since consideration of both conformations was not possible within a single calculation, the spectra for each conformer and its isotopologues were considered individually.

In the simulated spectra for gauche-ethanol (spectrum D, Figure 5), strong peaks due to the C–O ethanol stretch were observed at 1056–1064 cm⁻¹ for all three isotopologues, corresponding to the strong absorbance in the experimental spectrum at 1050 cm⁻¹ (spectrum B, Figure 4). In protic gauche-ethanol an absorbance due to vibrational mode B was observed at 1100 cm⁻¹, on the higher frequency side of the C–O stretch, corresponding to the strong absorbance at 1090 cm⁻¹ in the experiment, while the deuterated equivalent of this peak shifted down to 952 cm⁻¹, on the lower frequency side of the C–O stretch. This explains the appearance of the moderate peak at 950 cm⁻¹ (spectrum B, Figure 4, labeled in purple) and the corresponding decrease in intensity of the 1090 cm⁻¹ absorbance. The sharp absorbance at 880 cm⁻¹ in the experiment is accounted for by the peaks at 884–892 cm⁻¹ as a result of vibrational mode C.

In contrast, the simulated spectra for antiethanol (spectrum E, Figure 5) did not match up with the experimental spectra as closely. Although strong absorbances caused by the C–O ethanol stretch were observed for deuterated and tritiated antiethanol at 1076 and 1070 cm⁻¹, respectively, the same mode unexpectedly lowered to 1052 cm⁻¹ for protic antiethanol. Nevertheless, peaks corresponding to vibrational mode D, analogous to mode B, were observed moving from the high-frequency side of the C–O stretch for protic antiethanol (1104 cm⁻¹), to the lower frequency side for the deuterated equivalent (948 cm⁻¹). With respect to the experimental spectra, this accounts for the reduction in intensity of the peak at 1190 cm⁻¹ and the corresponding appearance of the moderate peak at 950 cm⁻¹ (spectrum B, Figure 4, labeled in purple) on addition of deuterium. No peak equivalent to vibrational mode C was observed.

By consideration of both conformations, extrapolation of these trends to tritiated ethanol would predict a further shift of the peak at 950 cm⁻¹ down to the region of 844–904 cm⁻¹. Given the superior match up of gauche-ethanol with experiment, and its double degeneracy relative to the anti conformation, a value on the lower end of this range would be more likely. Furthermore, the simulated gauche-ethanol spectra indicate that this peak would be distinct from the peak due to mode C (880 cm⁻¹ in experiment), making successful resolution more likely.

CONCLUSIONS

A novel ATR-FTIR based technique for quantifying the deuterium concentration in water has been developed. This technique has been validated at length and is robust to pH and ambient atmosphere while being less robust to the temperature and ionic strength of the water under test. In addition, a chemical signal amplification technique has been devised which increases the sensitivity of the technique by 2 orders of magnitude and with further work could be integrated into the method. Computational simulations have suggested that these techniques could be extended to the quantification of tritium concentrations in water. The availability of an inexpensive, readily available, nontoxic, and environmentally sound signal amplification chemical in the form of ethanol brings the sensitivity of ATR-FTIR into line with other much more

Table 3. Comparison of Available Techniques for Analysis of Deuterium in Water, This Work Highlighted in Green^a

technique	SD of δD determinations	advantages	issues
IRMS	2–5 ‰ ¹⁶	most stable isotopes quantifiable	complex sample preparation ^b
CRDS	0.40 ‰ ⁴⁰	sensitivity	complex sample preparation ^b
OA-ICOS	0.29 ‰ ⁴¹	sensitivity	complex sample preparation ^b
flow FTIR	38.54 ‰ ⁹	simple sample prep/instrumentation	sensitivity
ATR-FTIR-H ₂ O	273.53 ‰	simple sample prep/instrumentation	sensitivity
ATR-FTIR-EtOH	1.60 ‰	simple sample prep/instrumentation	requires ethanol contact with ATR cell

^aIRMS, isotope ratio mass spectrometry; CRDS, cavity ring-down spectroscopy; OA-ICOS, off-axis integrated cavity output spectroscopy; and ATR-FTIR, attenuated total reflectance–Fourier transform infrared spectroscopy. ^bGas phase sample, liquids require additional preparation.

complex and expensive techniques (Table 3), potentially allowing its use in any of the applications previously mentioned. As expected, substantial improvements to sensitivity are still required if it is to rival radiation based techniques such as LSC for the quantification of tritium in water streams; however, its ease of use and ability to provide data online and in flow may allow its use in some functions previously fulfilled by LSC. Although no testing was conducted with tritium, the simulated IR spectra suggest that its quantification should be possible in the same manner as deuterium.

■ ASSOCIATED CONTENT

SI Supporting Information

The Supporting Information is available free of charge at <https://pubs.acs.org/doi/10.1021/acs.analchem.9b05635>.

General considerations, details of method 1, method validation protocol, validation data, MATLAB algorithm, energies and molecular geometries of all computed structures, and hydrogen bonded and anharmonic simulated IR spectra (PDF)

■ AUTHOR INFORMATION

Corresponding Authors

Alfred K. Hill – Department of Chemical Engineering, University of Bath, Bath BA2 7AY, United Kingdom; orcid.org/0000-0003-4324-3822; Email: a.k.hill@bath.ac.uk

Ruth L. Webster – Department of Chemistry, University of Bath, Bath BA2 7AY, United Kingdom; orcid.org/0000-0001-9199-7579; Email: r.l.webster@bath.ac.uk

Authors

Cei B. Provis-Evans – Department of Chemistry and Centre for Sustainable Chemical Technologies, University of Bath, Bath BA2 7AY, United Kingdom; orcid.org/0000-0003-0309-3858

Elliot H. E. Farrar – Department of Chemistry, University of Bath, Bath BA2 7AY, United Kingdom; orcid.org/0000-0003-3350-2907

Matthew N. Grayson – Department of Chemistry, University of Bath, Bath BA2 7AY, United Kingdom; orcid.org/0000-0003-2116-7929

Complete contact information is available at:

<https://pubs.acs.org/doi/10.1021/acs.analchem.9b05635>

Notes

The authors declare no competing financial interest.

■ ACKNOWLEDGMENTS

The authors acknowledge UK Atomic Energy Authority, Nuclear Security Science Network (STFC 21st Century Global Challenge Network Project), EPSRC (RLW), Balena High Performance Computing Service (University of Bath), University of Bath DTP fund (EF), and Matthew Clarke, Callum Woolf, and Kartika Abdul Ghafar for experimental assistance.

■ REFERENCES

- (1) Geniesse, D. J.; Stegen, G. E. *Evaluation of Tritium Removal and Mitigation Technologies for Wastewater Treatment*, 2009.
- (2) Farid, O.; Shih, K.; Lee, W. E.; Yamana, H. *Fukushima: The Current Situation and Future Plans*, 2013.
- (3) Blowers, P.; Dale, C.; Dell, A. N.; Fletcher, N.; Frewin, P.; Green, N.; et al. *Guidance on the Measurement of Tritium in Environmental Samples*, 2005.
- (4) Nikolov, J.; Todorovic, N.; Jankovic, M.; Vostinar, M.; Bikit, I.; Veskovic, M. *Appl. Radiat. Isot.* **2013**, *71* (1), 51–56.
- (5) Galewsky, J.; Steen-Larsen, H. C.; Field, R. D.; Worden, J.; Risi, C.; Schneider, M. *Rev. Geophys.* **2016**, *54* (4), 809–865.
- (6) Bila, W. C.; Mariano, R. M. d. S.; Silva, V. R.; dos Santos, M. E. S. M.; Lamounier, J. A.; Ferriolli, E.; Galdino, A. S.; et al. *Isot. Environ. Health Stud.* **2017**, *53* (4), 327–343.
- (7) Sharp, Z. D.; Atudorei, V.; Panarello, H. O.; Fernández, J.; Douthitt, C. J. *Archaeol. Sci.* **2003**, *30* (12), 1709–1716.
- (8) Finlay, J. C.; Kendall, C. *Stable Isotope Tracing of Temporal and Spatial Variability in Organic Matter Sources to Freshwater Ecosystems*, 2008.
- (9) Litvak, I.; Anker, Y.; Cohen, H. *RSC Adv.* **2018**, *8* (50), 28472–28479.
- (10) Coplen, T. B. *Pure Appl. Chem.* **1994**, *66* (2), 273–276.
- (11) Hayes, F. N.; Gould, R. G. *Science* **1953**, *117* (3044), 480–482.
- (12) Clarke, W. B.; Jenkins, W. J.; Top, Z. *Int. J. Appl. Radiat. Isot.* **1976**, *27* (9), 515–522.
- (13) IAEA *Statistical Treatment of Data on Environmental Isotopes in Precipitation*, 1992.
- (14) De Groot, P. A. *Handbook of Stable Isotope Analytical Techniques* **2004**, *1*, ix.
- (15) Manian, S. H.; Urey, H. C.; Bleakney, W. J. *Am. Chem. Soc.* **1934**, *56* (12), 2601–2609.
- (16) Sessions, A. L. *J. Sep. Sci.* **2006**, *29* (12), 1946–1961.
- (17) Lehmann, B.; Wahlen, M.; Zumbunn, R.; Oeschger, H.; Schnell, W. *Appl. Phys.* **1977**, *13* (2), 153–158.
- (18) O'Keefe, A.; Deacon, D. A. G. *Rev. Sci. Instrum.* **1988**, *59* (12), 2544–2551.
- (19) Paul, J. B.; Lapson, L.; Anderson, J. G. *Appl. Opt.* **2001**, *40* (27), 4904.
- (20) Roth, E. *Pure Appl. Chem.* **1997**, *69* (8), 1753–1828.
- (21) Rao, M. S. *Stable Isotopic Analysis Using Mass Spectrometry and Laser Based Techniques: A Review*. In *Emerging Trends in Science, Engineering and Technology*; Sathiyamoorthy, S., Caroline, B. E., Jayanthi, J. G., Eds.; Springer: India, 2012; pp 523–538.
- (22) Kelly, S. D.; Parker, I. G.; Sharman, M.; Dennis, M. J. *J. Mass Spectrom.* **1998**, *33* (8), 735–738.

- (23) Donnelly, T.; Waldron, S.; Tait, A.; Dougans, J.; Bearhop, S. *Rapid Commun. Mass Spectrom.* **2001**, *15* (15), 1297–1303.
- (24) Wang, Y.; Sessions, A. L. *Anal. Chem.* **2008**, *80* (23), 9162–9170.
- (25) Thornton, V.; Condon, F. E. *Anal. Chem.* **1950**, *22* (5), 690–691.
- (26) Frisch, M. J.; et al. *Gaussian 16*, revision A.03; Gaussian, Inc.: Wallingford, CT, 2016.
- (27) Becke, A. D. *J. Chem. Phys.* **1993**, *98* (7), 5648–5652.
- (28) Stephens, P. J.; Devlin, F. J.; Chabalowski, C. F.; Frisch, M. J. *J. Phys. Chem.* **1994**, *98* (45), 11623–11627.
- (29) Grimme, S.; Ehrlich, S.; Goerigk, L. *J. Comput. Chem.* **2011**, *32* (7), 1456–1465.
- (30) Weigend, F.; Ahlrichs, R. *Phys. Chem. Chem. Phys.* **2005**, *7* (18), 3297.
- (31) Mennucci, B.; Cammi, R.; Tomasi, J. *J. Chem. Phys.* **1998**, *109* (7), 2798–2807.
- (32) Funes-Ardoiz, I.; Paton, R. S. Goodvibes: Version 2.0.3. 2018.
- (33) Shalem, S.; German, A.; Barkay, N.; Moser, F.; Katzir, A. *Fiber Integr. Opt.* **1997**, *16* (1), 27–54.
- (34) International Conference on Harmonization (ICH). Guidance for Industry: Q2B Validation of Analytical Procedures: Methodology. 1996.
- (35) Shabir, G. J. *Valid. Technol.* **2004**, *10*, 210–218.
- (36) Rohman, A.; Musfiroh, A.; Wijaya, E. G. *Glob. J. Pharmacol.* **2013**, *7* (3), 270–275.
- (37) Perevezentsev, A. N.; Bell, A. C.; Brennan, P. D.; Hemmerich, J. L. *Fusion Eng. Des.* **2002**, *61* (62), 585–589.
- (38) Janković, M. M.; Todorović, D. J.; Keleman, Z.; Miljević, N. R. *Nucl. Technol. Radiat. Prot.* **2012**, *27* (3), 239–246.
- (39) Scheiner, S.; Seybold, P. G. *Struct. Chem.* **2009**, *20* (1), 43–48.
- (40) Skrzypek, G.; Ford, D. *Environ. Sci. Technol.* **2014**, *48* (5), 2827–2834.
- (41) Lis, G.; Wassenaar, L. I.; Hendry, M. J. *Anal. Chem.* **2008**, *80* (1), 287–293.